Ionization of C_{70} and C_{60} molecules by slow highly charged ions: A comparison

J. Jensen, H. Zettergren, H. T. Schmidt, and H. Cederquist
Physics Department, Stockholm University, AlbaNova University Center, S-106 91 Stockholm, Sweden

S. Tomita, S. B. Nielsen, J. Rangama, and P. Hvelplund
Department of Physics and Astronomy, University of Aarhus, DK-8000 Aarhus C, Denmark

B. Manil and B. A. Huber
CIRIL/GANIL, rue Claude Bloch, Boîte Postale 5133, F-14070 Caen Cedex 05, France
(Received 3 December 2003; published 18 May 2004)

We have studied collisions between slow highly charged ions and pure C_{70} and C_{60} molecular targets, and report on measurements of target ionization and fragmentation in electron transfer processes. The intensity distributions in the fragmentation spectra for C_{60} and C_{70} are rather similar, indicating that similar roles are played by evaporation (neutral C_2 emission) and fission processes (charged particle emission) in the two systems. For C_{70}, intact molecular ions are formed in charge states up to 10+, while the maximum charge state for C_{60} molecules is 9+ following collisions with Xe^{23+} at 69 keV. The kinetic-energy releases measured for asymmetric fission of C_{70} ions ($C_{70}{}^{r+} \rightarrow C_{68}{}^{(r-1)} + C_2{}^+$) are mostly close to the corresponding ones for C_{60}, while both sets of results are significantly lower than those reported for electron-impact ionization studies of C_{60} and C_{70}. Kinetic-energy releases and fission barrier heights are estimated for C_{60} and C_{70} ions using an electrostatic model. An increased intensity of the higher charge states of C_{70} ions is observed compared to the C_{60} case, which most likely is due to a larger number of degrees of freedom on which the internal excitation energy may be distributed.

DOI: 10.1103/PhysRevA.69.053203 PACS number(s): 36.40.Qv, 34.70.+e, 36.40.Wa

I. INTRODUCTION

Over the past decade a vast number of collision experiments using C_{60} molecules as targets and different types of projectiles have been carried out [1–15]. The creation of multiply charged C_{60} ions and the investigation of the subsequent decay processes have been used to probe fullerene stabilities and dynamics. Fragmentation of collisionally excited fullerenes depends on their internal energies, the mobility of the valence electrons, and the couplings of electronic and vibrational degrees of freedom. The energetics and dynamics of dissociation reactions of neutral and charged C_{60} have been studied extensively using different experimental methods. In particular, the energy deposition in clusters has been analyzed through the kinetic-energy releases (KER) [4,5,7,9–15] in the various dissociation processes, and by investigations of the balance in the production of intact and fragmented C_{60} ions [3,14,15].

Collisions involving higher fullerenes, such as C_{70}, have been studied to a much smaller extent. One may ask what happens as the number of atoms and thus the number of degrees of freedom over which the internal energy can be distributed increase, and how does the response to the external perturbation change? The ionization and fragmentation of the C_{70} molecule have mainly been investigated using electron bombardment [2,9,10,13,16–20] and photon irradiations [1]. There are a few studies on ion formation and degradation of C_{70} by gas-phase fast-atom bombardment using keV neutral atoms [21,22], and there are also some collision studies using C_{70} ions as projectiles investigating fragmentation and electron capture [23–26]. However, experiments in which atomic ions collide with C_{70} are scarce, and then only mixed C_{70}/C_{60} targets have been used, obscuring the picture of the C_{70} fragmentation processes. Jin *et al.* [27] found that $C_{60}{}^{r+}$ with r up to 9 is formed in collisions between Bi^{44+} and C_{60} at 500 keV. As a mixture of C_{60} and C_{70} was used, also several peaks corresponding to intact C_{70} ions in charge states up to 6+ were observed [27]. This is also, to our knowledge, the highest charge state of C_{70} found in electron bombardment studies up to this date [10,16].

Multiply charged cluster ions are produced efficiently in slow ($v \ll 1$ a.u.) collisions between highly charged ions and clusters [3,28,29]. At low collision energies, electron capture dominates the interaction, and the capture process occurs already at large distances, and only limited amounts of energies are transferred to internal nuclear motion and electronic excitations [28]. In collisions with projectiles in lower charge states, the interaction processes are dominated by smaller impact parameters leading to higher target electronic and vibrational excitations.

In this work, we present, to our knowledge, the first experimental results on the ionization and fragmentation following slow collisions between highly charged ions and a *pure* C_{70} target. This will be compared with results for C_{60}. The multiply charged C_{70}, or C_{60}, ions are produced in $Xe^{q+} + C_{70}/C_{60} \rightarrow Xe^{(q-s)+} + C_{70}{}^{r+}/C_{60}{}^{r+} + (r-s)e^-$ collisions at $3q$ keV by electron capture processes. Here, q is the projectile charge state ($q=8$, 16, and 23), r is the number of electrons removed from the fullerene, and s is the number of electrons stabilized on the projectile.

In Sec. II, we describe the experimental technique, while we present fragmentation intensity distributions and KER values for C_{70} and C_{60} in Sec. III. The present experimental results for asymmetric fission ($C_2{}^+$ emission) are qualita-

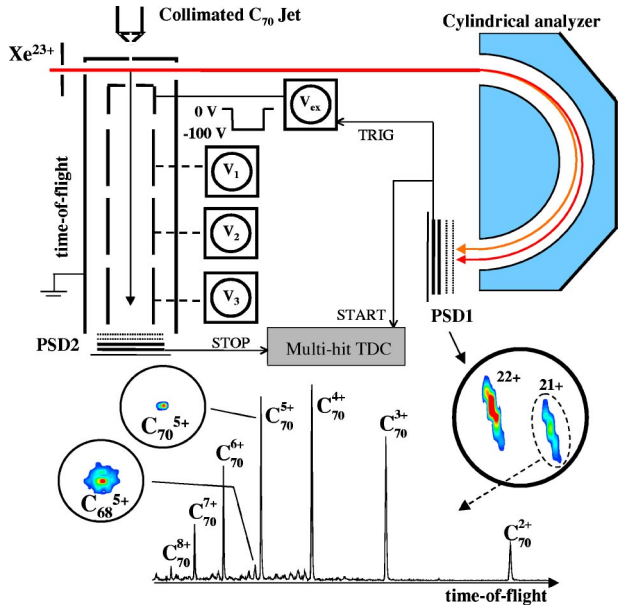

FIG. 1. A schematic of the setup used for coincidence registration of final projectile and target charge states and the fragment kinetic energies. An example of 69 keV Xe^{23+} ions colliding with C_{70} is shown. The analyzer voltage is set such that only Xe^{22+} and Xe^{21+} ions hit the position sensitive detector (PSD1). The corresponding image on the detector is shown as an inset. The time-of-flight distribution of the recoil ions coincident with the outgoing Xe^{21+} ions ($s=2$) are also shown and for each one of the peaks in this spectrum there is a corresponding image on PSD2. Examples are displayed for $C_{70}{}^{5+}$ and $C_{68}{}^{5+}$.

tively explained in Sec. IV by an electrostatic model [30,31] in which we assume that C_{70}, C_{60} and their fragments may be treated as conducting spheres. In Sec. IV we also discuss evidences for the production of $C_{70}{}^{10+}$, while there is no indication of intact $C_{60}{}^{10+}$ ions under identical experimental conditions. We will argue that the higher stability for C_{70} is due to the possibility to distribute the internal energy on a larger number of vibrational modes.

II. EXPERIMENT

The experimental method is described in detail elsewhere [14,15], and only a brief description is given here. The highly charged atomic projectiles (Xe^{8+}, Xe^{16+}, and Xe^{23+}) were produced in the 14.5 GHz Electron Cyclotron Resonance (ECR) ion source at the Manne Siegbahn Laboratory, Stockholm University. The ions had energies of $3q$ keV and the ion beam was collimated before entering the experimental setup shown in Fig. 1. The beam crossed collimated C_{70} or C_{60} jets, effusing from a small oven. The temperature of the oven was set to 600 °C for both targets. The C_{60} and C_{70} powders had purities of 99.9% and 99.4% (Hoechst), respectively (0.4% of the C_{70} powder consist of C_{60}, and 0.2% consist of higher fullerenes). The oven was carefully cleaned between target changes. The interaction region lies in the extraction stage of a linear time-of-flight mass spectrometer, and the fullerene jets point in the direction of the spectrometer axis.

Projectile ions exiting the collision chamber in the $(q-s)+$ charge state (i.e., stabilizing s electrons) were selected by means of a 180° electrostatic cylindrical analyzer followed by a position sensitive detector (PSD1). A fast signal from the projectile detector triggered a transverse electric field, which extracted fullerene recoil ions towards the drift region of the time-of-flight spectrometer with a position sensitive detector (recoil detector with 50 mm diameter, PSD2). The multiply charged fullerenes and their fragments were analyzed with respect to their time of flights, determined by the "start signals" from the projectile (which also triggered the extraction) and the "stop signals" from the recoil detector. Note that this method gives a delay—the time it takes the projectile to reach its detector (roughly 1 μs)—between the ionization of a target molecule and its extraction. The data were stored event by event in list mode using a multihit time-to-digital converter . However, due to limited fullerene detection efficiencies (the front of PSD2 was floated on −3 kV) only few multiple hits were registered. The time-of-flight spectra shown in the following are thus dominated by single-hit events. One example is shown in Fig. 1 where charged fragmentation products and ions of C_{70} were recorded in coincidence with two electrons stabilized on Xe^{23+} projectiles. Time-of-flight peaks are associated with position distributions (on PSD2) characteristic for kinetic-energy releases in the postcollisional fragmentation processes. The method to extract KER values has been discussed in detail earlier [14,15].

III. RESULTS

A. Mass spectra

For the C_{60} target it has been demonstrated [28,32,33] that the fragmentation depends on the energy deposited in the C_{60} molecule. By increasing the internal energy of C_{60} above a certain threshold the initially dominating fragmentation channel, loss of C_2 molecules, is overtaken by breakups of the cage into linear chains and rings of carbon atoms [32]. The internal fullerene energy resulting from a collision varies as a function of the impact parameter which can be selected roughly through the number of electrons removed from the fullerene target (r). Thus the fragmentation pattern depends on r [34]. In addition, there is a correlation (although less strong) between impact parameter and the number of stabilized electrons (s). A correlation between the number of active electrons from a C_{60} target and the number stabilized on the projectile has been observed [35,36].

In Fig. 2 we compare mass spectra for 24 keV Xe^{8+} collisions with C_{70} (left) and C_{60} (right). The spectra were taken in coincidences with one ($s=1$, upper spectra) and two ($s=2$, lower spectra) stabilized electrons on the projectiles. First, we note that the $C_{60}{}^{3+}$, $C_{60}{}^{4+}$, and $C_{60}{}^{5+}$ peaks in the C_{70} spectrum ($s=2$) are due to fragmentation of C_{70} ions, and not to impurities in the C_{70} jet. This is seen by comparing two-dimensional position distributions on the recoil detector for, e.g., $C_{60}{}^{3+}$ (see insets of Fig. 2). The $C_{60}{}^{3+}$ ions coming from the fragmentation of C_{70} ions have wider distributions than $C_{60}{}^{3+}$ ions created directly by soft electron removal

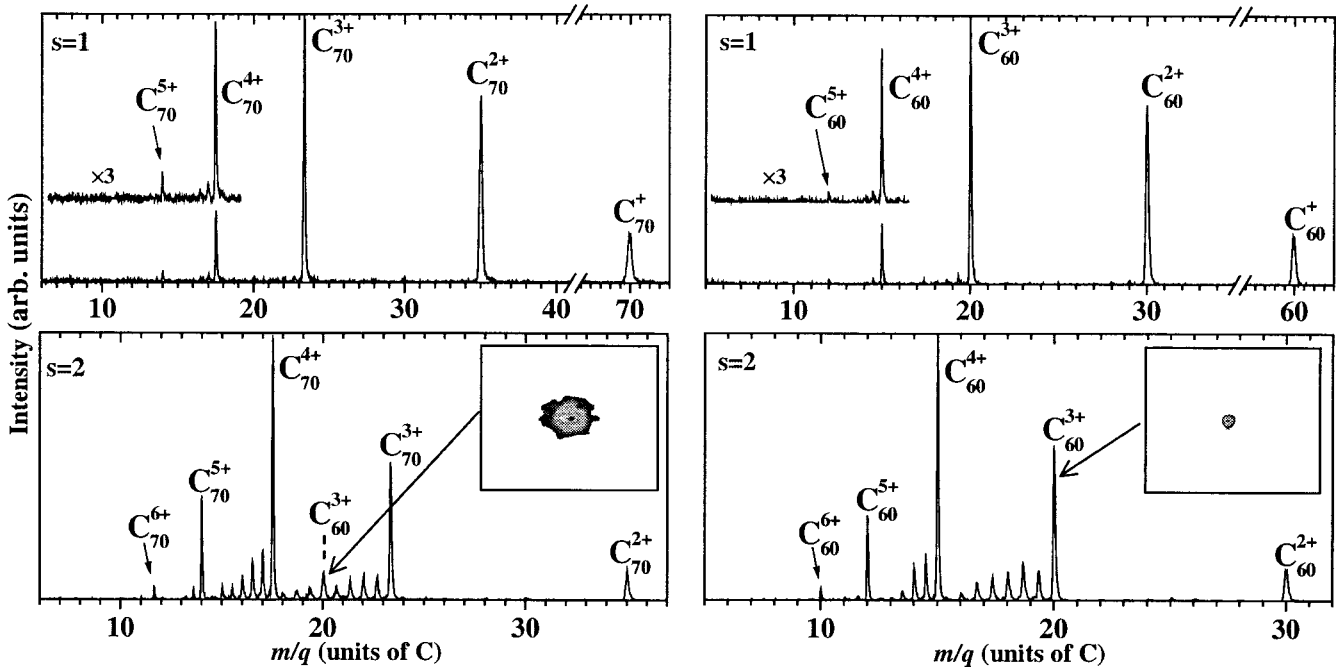

FIG. 2. Mass spectra from 24 keV Xe^{8+}-C_{70} collisions (left) and 24 keV Xe^{8+}-C_{60} collisions (right). The upper spectra are taken in coincidence with one electron stabilized on the projectiles ($s=1$), and the lower with two stabilized electrons ($s=2$). Position distributions on the recoil detector of the $C_{60}{}^{3+}$ ions are shown as insets. The dimensions of the detector images are 16×16 mm^2, which are only smaller parts of the whole detector area (50 mm in diameter).

from neutral C_{60} molecules. Similar observations are made for $C_{60}{}^{4+}$ and $C_{60}{}^{5+}$ ions. The strong C_{60} fragment production for the C_{70} target, where fragmentation processes given by asymmetric fission and evaporation dominate, is due to the exceptional stability of the C_{60} molecule as compared to, e.g., C_{58} or C_{62}. This means that sequential evaporation and/or fission processes are likely to result in C_{60} ion production. The $C_{60}{}^{2+}$ contribution in the C_{70} ($s=2$) spectrum is extremely small and consistent with the 0.4% C_{60} content of the C_{70} powder. In addition, they show a narrow distribution on the recoil detector, characteristic for intact ions. The C_{60} and C_{70} mass spectra are similar, except for an enhanced production of $C_{70}{}^{5+}$ ($s=1$) compared to $C_{60}{}^{5+}$ ($s=1$) as shown in the upper two spectra. The intensity ratios between the highest observed charge states, 5+ and 4+, is 0.14 ± 0.01 and 0.08 ± 0.01 for C_{70} and C_{60}, respectively. Also, $C_{70}{}^{5+}$ seems to be stronger than $C_{60}{}^{5+}$ in the $s=2$ spectra. The present 24 keV Xe^{8+}-C_{60} spectra are almost identical to the results reported for 24 keV Ar^{8+}-C_{60} collisions as can be seen from a comparison with Figs. 1 and 22 in Ref. [3] and [28], respectively. This indicates that direct vibrational excitation from distant elastic collision processes (which should be different for Ar and Xe projectiles at the same energy) is relatively unimportant at the present velocities, impact parameters, and projectile charge states.

Going to higher projectile charge states, the critical distances for electron transfer increase. This leads to colder target ions yielding less fragmentation and higher charge states of intact C_{70} and C_{60}. In Fig. 3, we show the ionization and fragmentation patterns of C_{70} and C_{60} recorded in coincidence with outgoing projectiles stabilizing one, two, and three electrons ($s=1-3$) in collisions with 69 keV Xe^{23+}-projectile ions. For $s=1$, mainly intact C_{70} and C_{60} ions in charge state up to seven are seen. Events with $s=1$ are mostly associated with large impact parameters, where several electrons are gently extracted from the target in over-the-barrier electron capture processes, and finally only one of them is stabilized while the others are lost through autoionization from the projectile. This leads to the creation of comparatively cold and stable target molecular ions.

For outgoing Xe^{21+} ($s=2$) mostly intact molecules with charge states up to 9+ are observed, but the fragmentation increases slightly (as compared to the $s=1$ cases) as seen in the sequences of peaks to the left of $C_{70}{}^{3+}$, $C_{70}{}^{4+}$, and $C_{70}{}^{5+}$ in (a), and $C_{60}{}^{3+}$, $C_{60}{}^{4+}$, and $C_{60}{}^{5+}$ in (b). These peaks stem from the break-ups of $C_{70}{}^{r+}$ and $C_{60}{}^{r+}$ ions with $r\geqslant3$. The corresponding heavy fullerene fragments (C_{70-2m} and C_{60-2m}) with rather low intensities are thus produced in charge states larger than or equal to three and with even numbers of carbon atoms ($70-2m=68,66,64,\ldots$, or $60-2m=58,56,54,\ldots$). These $s=2$ events are mainly due to fullerene ions produced in intermediate impact parameter collisions resulting in internal energies, such that light neutral, or charged, small fragments are emitted.

The amount of fragmentation increases for coincidences with outgoing Xe^{20+} ions ($s=3$), and light singly charged fragments become competitive in intensity with the heavier fragments. The increased multifragmentation indicates that intact C_{60} and C_{70} of higher charge states than observed directly in the mass spectra may be produced to larger extents [35,36] (but with short lifetimes), as multifragmentation is important for the destruction of C_{60} when $r>6$ [34]. Events with $s>3$ are on the average associated with smaller impact parameters where the projectile passes close to the cage lead-

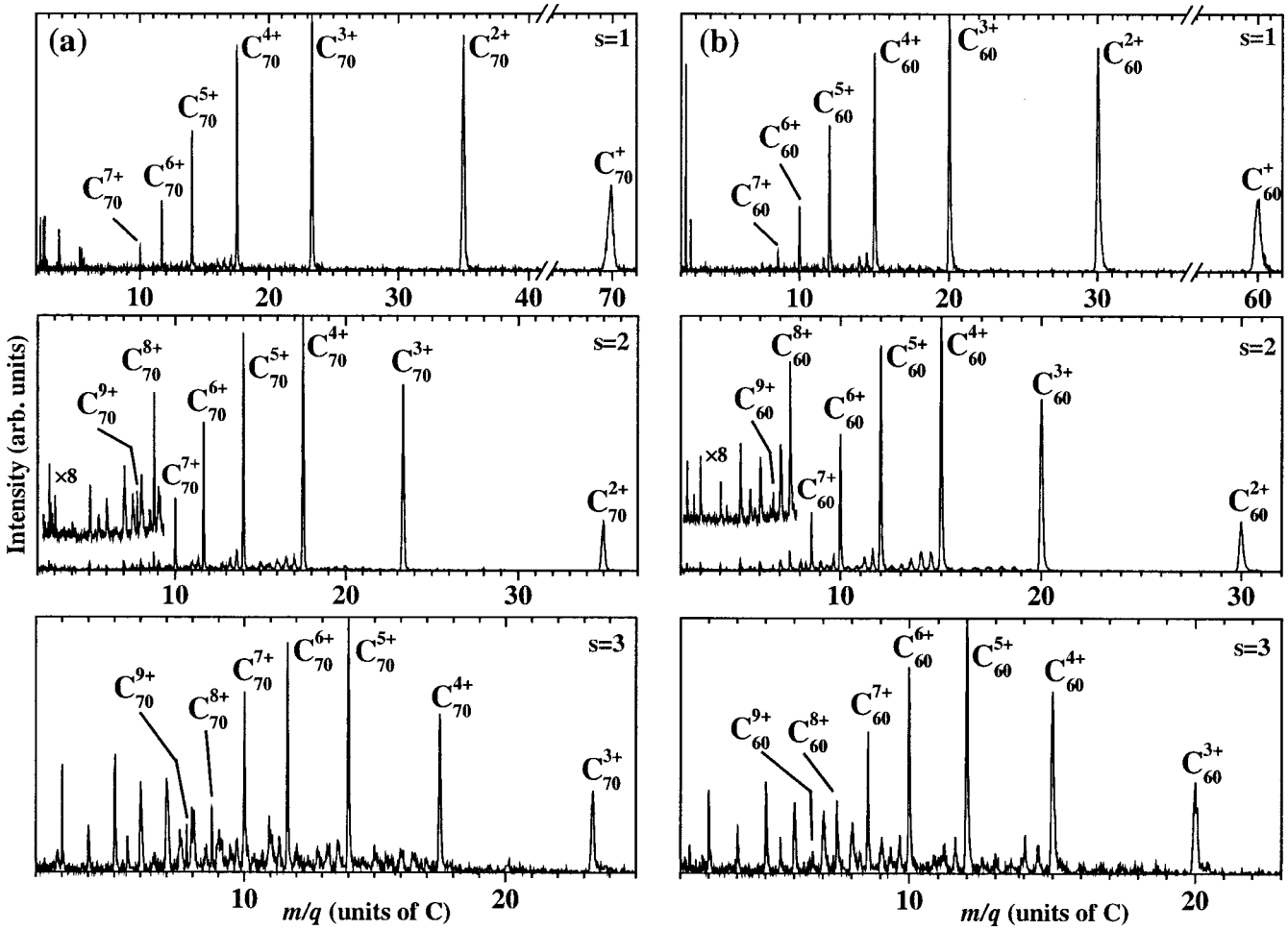

FIG. 3. The mass distribution of recoiling intact and fragmented fullerene ions measured in coincidence with $s=1-3$ electrons stabilized on 69 keV Xe^{23+} projectile ions after collision with (a) C_{70} and (b) C_{60}.

ing to higher internal energies and possibly to destruction of the fullerene cages into even and odd numbered light fragments. For $s=4$ (not shown) we do not detect any intact C_{60} or C_{70} ions.

In Fig. 4(a), we show the Xe^{23+}-C_{70} ($s=3$) spectrum extended in m/q up to $r=1$, demonstrating that there is only a small contamination due to multiple collision events involving capture of one and two electrons from C_{70} ($r=1$ and $r=2$). For $s=2$ there is no contamination at all from $r=1$ events. Figure 4(b) shows the Xe^{23+}-C_{70} ($s=3$) spectrum in more detail. Doubly charged carbon clusters are now also clearly visible, as well as intact C_{70} molecular ions in charge states up to (at least) 9+. The intensity distribution of singly and doubly charged light fragments (i.e., C_n^+ and C_n^{2+}) is almost identical for the C_{70} and C_{60} targets (the latter ones are not shown).

In Fig. 4(d) we discriminate between hits on the position sensitive recoil detector corresponding to intact and fragmented fullerene ions. As the fragmented C_{70} ions have much broader position distributions than the intact ones [see Fig. 4(c)], we obtain a mass spectrum almost free of fragments by selecting central hits on the recoil detector. This indicates the production of intact $C_{70}{}^{10+}$ ions. No such clear indication of intact 10+ ions was found for C_{60} under exactly the same conditions (Xe^{23+} projectiles at 69 keV) or with other highly charged Xe ions [15]. Brenac *et al.* [37] have, however, reported indications of intact $C_{60}{}^{10+}$, using slow highly charged ions, but under somewhat different experimental conditions. In Table I, we show measured $C_{70}{}^{9+}/C_{70}{}^{8+}$ and $C_{60}{}^{9+}/C_{60}{}^{8+}$ intensity ratios for one through three stabilized electrons ($s=1-3$). These ratios are significantly higher in all three cases for C_{70} than for C_{60}. These observations signal a higher stability for $C_{70}{}^{9+}$ than for $C_{60}{}^{9+}$ and it is thus not surprising that the $C_{70}{}^{10+}$ ions survive the time-of-flight to much larger extents than $C_{60}{}^{10+}$ (i.e., enhanced intensity of $C_{70}{}^{10+}$ ions in accordance with Fig. 4). In Fig. 5, we show apparent production cross sections for intact C_{60} and C_{70} ions. The relations between the $s=1$, $s=2$, and $s=3$ curves have been established through the measured projectile charge state distributions. Except for the noted difference at high r, the recoil charge state dependencies are strikingly similar.

B. Kinetic-energy releases

Fullerene fragments which are due to C_2^+ ion emission from C_{70} or C_{60} have a broader position image on the recoil detector than their nondissociative counterparts due to the

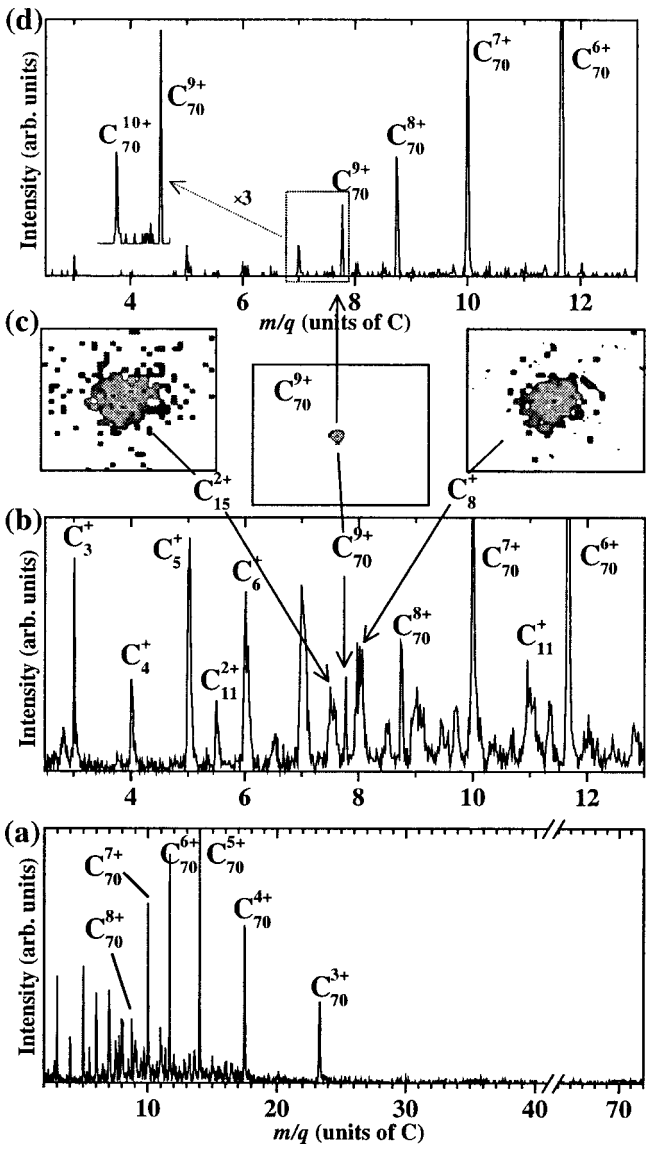

FIG. 4. (a) The mass spectrum for $s=3$ in Xe^{23+}-C_{70} collisions. (b) Details of the mass spectrum in (a), where the C_{70}^{9+} peak is clearly seen. (c) Position distributions on the recoil detector for C_{70}^{9+}, C_8^+, and C_{15}^{2+} ions. The dimensions of the detector images are 16×16 mm^2. (d) This spectrum is obtained after selecting (central) hits on the recoil detector corresponding mainly to intact C_{70} ions exposing a significant C_{70}^{10+} contribution. The intensity axis in (b) and (d) are 50% of the one in (a).

substantial energy release in the dissociation process [14,15]. From the widths of the fragment ion peaks it is possible to deduce the kinetic recoil energies of, e.g., C_{58} (from C_{60}) and C_{68} (from C_{70}) ions, and to use simple kinematics to obtain the corresponding kinetic-energy releases. The method to extract KER values, including the calibration method using room-temperature Xe target gas, is described in detail in earlier work [14,15]. The resulting resolution for the KER measurements using this method is ~0.1 eV (see Ref. [15]). The present KER results are shown together with some literature values in Fig. 6 for the processes in which C_{70}^{r+} or C_{60}^{r+} emits a single C_2^+ molecule as a function of the initial fullerene charge state r. Also shown are KER values obtained by the present technique for the process where C_{60}^{r+} emits a single C_2^+ molecule after collision with 50 keV Xe^{17+} ions [15]. In Table II we summarize the present kinetic-energy release measurements for asymmetric fission of C_{70} ions following Xe^{16+} and Xe^{23+} collisions. The KER values increase as functions of r, and they are similar for the two projectiles and the C_{60} and C_{70} targets.

TABLE I. Ratios between charge states 9+ and 8+ produced by 69 keV Xe^{23+} projectiles for C_{70} and C_{60} as functions of the number of stabilized electrons s. Shown are also the corresponding ratios for the total charge state distribution.

	$s=1$	$s=2$	$s=3$	Total
C_{70}^{9+}/C_{70}^{8+}	0.13±0.05	0.20±0.03	0.42±0.07	0.19±0.04
C_{60}^{9+}/C_{60}^{8+}	0.08±0.04	0.13±0.02	0.20±0.05	0.12±0.02

The results shown in Table II and Fig. 6 are those for which $r\geqslant5$ and where we find that asymmetric fission (C_2^+ emission) dominates strongly over neutral C_2 emission. For lower $r(\leqslant4)$ we find significant and even dominating contribution from neutral C_2 emission. The KER values corresponding to the latter processes are indeed measured [14] (and found to be much lower than for C_2^+ emission) but are not the topic of the present paper. In the few cases where the contributions from C_2 and C_2^+ emission are similar, separate position distributions on the recoil detector (PSD2) may be distinguished.

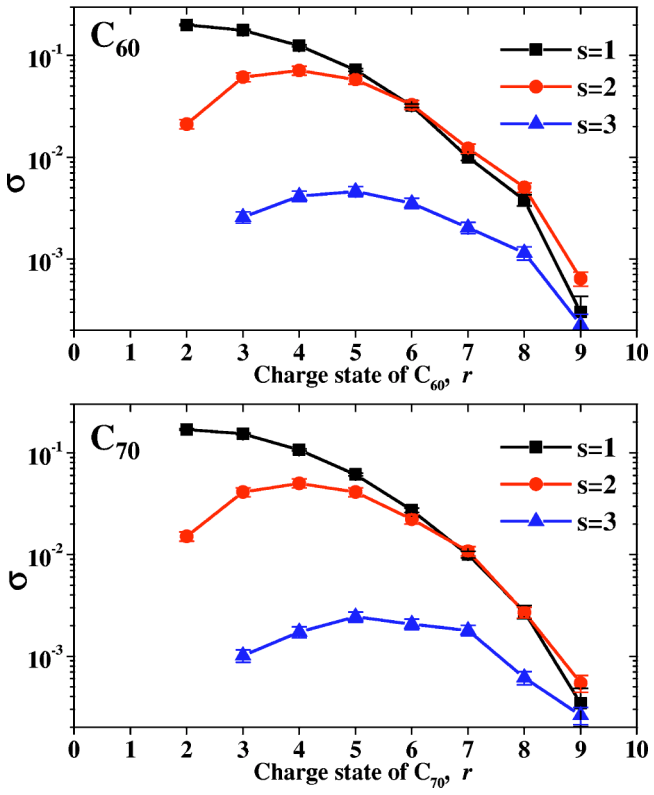

FIG. 5. Apparent cross sections for producing intact C_{60} (above) and C_{70} ions (below) with 69 keV Xe^{23+} ions.

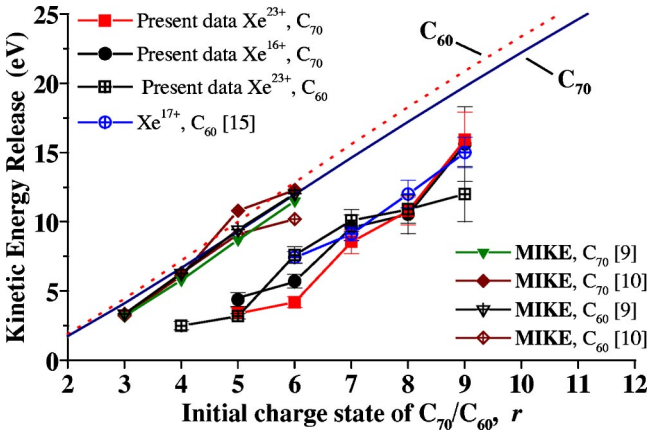

FIG. 6. Comparison between experimental KER values for processes where C_{70}^{r+} and C_{60}^{r+} emit a single C_2^+ ion as functions of the initial charge state. Some earlier measurements are based on the MIKE technique by Matt *et al.* [9] and Senn *et al.* [10]. The C_{60} data by Cederquist *et al.* [15] are obtained using the present technique and Xe^{17+} projectile ions. Also shown are calculated KER values for the fission process where a C_{70}^{r+} (full curve) or C_{60}^{r+} (dotted curve) ion emits a single C_2^+ ion. The model results are based on the interaction between two polarizable spheres of finite radii (see the text).

IV. DISCUSSION

A. Other experimental results on KER

In this section we will compare the present experimental results on kinetic-energy releases with earlier measurements using partly different techniques and fullerene ion production methods. In the MIKE scan technique (mass-analyzed ion kinetic energies) [9,10], the energy distributions of the heavy fragments (C_{58} and C_{68} ions) are measured by means of an electrostatic analyzer yielding KER values following electron impact ionization of C_{60} and C_{70}. In those measurements (Senn *et al.* [10] and Matt *et al.* [9]), the selected dissociation process is that of pure asymmetric fission, of the types $C_{60}^{r+}/C_{70}^{r+} \rightarrow C_{58}^{(r-1)+}/C_{68}^{(r-1)+}+C_2^+$. We note that the results of Senn *et al.* [10] and Matt *et al.* [9] (for which no error bars are given) are several standard deviations larger than the present results.

At present, the reason for this deviation is not clear, but a few differences between the experiments should be noted. First, the excitation methods are different yielding possible differences in internal temperatures just after the ionization process. Most likely the initial fullerene ions are colder after electron capture, but on the other hand, the decay is measured after delays of the order of 10 μs (depending on the charge state) in the MIKE experiments [9,10], and during this time cooling may occur [38]. In our experiment, the time delay between ion creation and extraction of the resulting fission fragments is typically of the order of 1 μs. Thus, the internal energies of the fullerene ions are quite different in the two experiments. However, this should influence the fission rate but should have less or no effect on the kinetic-energy release [4]. Second, while asymmetric fission and evaporation are unambiguously separated in the MIKE experiments we are only able to extract separate values with high confidence if the two channels have markedly different intensities (which most often is the case) [14]. The comparison with the MIKE data is further complicated by the fact that some earlier MIKE measurements on C_{60} [4] are consistent with our present result but in disagreement with the MIKE result shown in Fig. 6. We also note that the KER results for C_{60} by Tomita *et al.* [12] and Chen *et al.* [7], using electron capture to highly charged ions (and prompt excitations of the cluster ions as in the present experiments). yield results consistent with the present C_{60} data and Ref. [15].

TABLE II. Experimental KER values (given in eV) for the asymmetric fission process $C_{70}^{r+} \rightarrow C_{68}^{(r-1)+}+C_2^+$ using Xe^{16+} and Xe^{23+} projectiles.

	$r=5$	$r=6$	$r=7$	$r=8$	$r=9$
Xe^{16+}	4.4±0.5	5.7±0.5	9.6±0.9	10.5±1.4	15.6±2.7
Xe^{23+}	3.4±0.4	4.2±0.4	8.6±0.9	10.8±1.0	15.9±2.0

B. Comparisons with KER model results

An understanding of the mechanisms for asymmetric fragmentation processes has been developed by assuming that the internal energy is statistically distributed among all the degrees of freedom. A dissociation channel is open when a critical energy is accumulated on the associated reaction coordinate [33,39]. Here a simple statistical evaporation model, the so-called RRK theory developed by Rice, Ramsperger, and Kassel [40,41], was used. In addition, Märk *et al.* [4,5] have presented a dynamical picture for asymmetric fission of C_{60}^{r+} and other fullerene ions. To interpret the observed energy release of the fission channels $C_{60}^{r+}/C_{70}^{r+} \rightarrow C_{58}^{(r-1)+}/C_{68}^{(r-1)+}+C_2^+$, Märk *et al.* [4] proposed a two-step reaction sequence for the loss of a C_2^+ ion initiated by the unimolecular C_2 evaporation followed by a charge transfer from the neutral outgoing C_2 to the residual fullerene ion. This is known as the autocharge transfer (ACT) process. Recently, it has, however, been argued [12,15] that KER values for asymmetric fission of C_{60}^{r+} ions may be understood without the ACT mechanism (at least for higher charge states). Instead it appears that evaporation and asymmetric fission in general are independent processes governed by activation energies for neutral C_2 emission and fission barriers for C_2^+ emission.

In the model calculation (the results are shown in Fig. 6) we have assumed that the two separating fragments are conducting and rigid spheres and we calculate KER values following Zettergren *et al.* [30] (see also Näher *et al.* [42]). As this model also yields critical distances for over-the-barrier electron transfer between the fragments [30], we conclude that the ACT process most likely is inactive for the fission of C_{70} (which was also concluded earlier for the C_{60}^{r+} case [15]). It is interesting to note that this simple model predicts close KER values for C_{60} and C_{70} as observed in the present experiment and in the one based on the MIKE technique using electron bombardment. In fact, the latter experimental results are very close to the present model values. We be-

lieve, however, that this agreement to some extent is fortuitous as the model is extremely simple ignoring, e.g., effects of changes in the finite internal excitations of the fragments; that is, the possibility that charge separation (fragmentation) is accompanied by simultaneous internal excitations (i.e., fragments taking up some of the energy released) has to be taken into account [43]. This results in the final (excited) states having higher energies yielding smaller differences in relations to the maxima of the barriers, and a thereby smaller KER values. Still, the present simple model clearly gives the correct trend.

The model kinetic-energy releases in Fig. 6 are considered to be the differences between the interaction energies for infinite separation (assumed to be zero), and the maxima of the barriers of the potential-energy curves for the sphere-sphere interaction. The model potential energy $U_{\rm int}(R)$ for the spheres, at the center-center distance $R > a^H + a^L$, where a^H is the radius of the heavy (C_{68} or C_{58}) and a^L the radius of the light fragment (C_2), is given by

$$U_{\rm int}(R) = \frac{1}{2}\left[\frac{q^H(q_0^H - q^H)}{a^H} + \frac{q^L(q_0^L - q^L)}{a^L} \right], \qquad (1)$$

where q^H and q^L are the net sphere charges of the heavy and light fragments, respectively, while q_0^H and q_0^L are their center charges [30,31]. The center charges depend on the infinite number of image charges induced in the spheres and are functions of both net charges, the sphere radii, and R [30]. We have assumed the same surface density for C_{68} as for C_{60}, yielding $a^{\rm H} = a_{C68} = a_{C60}(1+8/60)^{1/2} = 7.66a_0$. The C_{60} radius $a_{C60} = 7.2a_0$ was obtained by fitting $I_r(C_{60}) = W + (r - 1/2)/a_{C60}$ to the experimental ionization potential for C_{60} [30,44], yielding also a value for the work function $W = 5.7$ eV. The radius $a^{\rm L} = a_{C2} = 2.38a_0$ of the C_2 fragment is deduced from $I_1(C_2) = W + 1/(2a_{C2})$ using the accepted experimental I_1 value 11.4 ± 0.4 eV [45]. For C_{70} we get $a_{C70} = a_{C60}(1+10/60)^{1/2} = 7.8a_0$. The ratio between this radius and the one for C_{60} is in accordance with recent measurements on the static polarizabilities of C_{70} and C_{60} [46]. Furthermore, calculating the first five ionization potentials for C_{70}, $I_r(C_{70}) = W + (r - 1/2)/a_{C70}$, we find good agreement with experimental results [19,47]. This shows that this simple surface density scaling and basic electrostatics describe sizes, polarizabilities, and ionization potentials rather well. The model energy releases for C_{60}^{r+} are obtained using a radius for the C_{58} ions of $7.1a_0$ [14,15].

C. Estimated fission barriers for C_{70} and C_{60} ions

The detection of intact multiply charged fullerene ions requires low internal energies of the ionized fullerenes and short experimental time windows, so that the fullerene ions can survive the analyzing time of several microseconds. A zero fission barrier height leads to immediate "Coulomb explosion", but a fullerene ion with nonzero fission barrier may also undergo fragmentation on the experimental time scale, even though it remains stable over many vibrational periods (picosecond time scale). The lower the internal energy is, the lower the fission barrier can be for a system avoiding fragmentation during the time of flight. The measured mass distributions are thus sensitive to lifetimes for intact fullerenes, which of course are related to their stabilities.

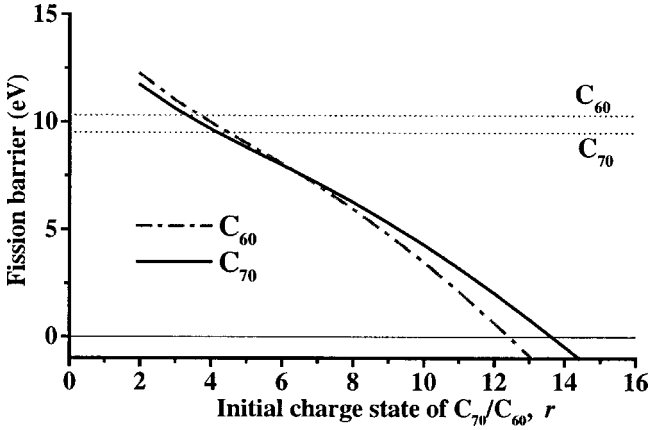

FIG. 7. Model fission barriers for the processes $C_{60}^{r+}/C_{70}^{r+} \rightarrow C_{58}^{(r-1)+}/C_{68}^{(r-1)+} + C_2^+$. The horizontal lines show the activation energy for neutral C_2 emission from C_{60} and C_{70} (here assumed to be independent of r).

The kinetic-energy releases, $E_{\rm KER}$, in asymmetric fission depend on fission barriers $B_{\rm fis}^r$ for emission of C_2^+, through [12,15,31]

$$B_{\rm fis}^r = E_{\rm KER} + E_a^{r-1} + I_1(C_2) - I_r(C_{70}/C_{60}), \qquad (2)$$

under the assumption that the internal excitation is unchanged during the fragmentation process. The activation energies for neutral C_2 emission (evaporation) from $C_{70}^{(r-1)+}$ or $C_{60}^{(r-1)+}$ are denoted E_a^{r-1}. In order to obtain information on the stability of C_{70}^{r+} and C_{60}^{r+} ions reliable data are needed for E_a^r and the ionization potentials I_r for C_2 and C_{70}/C_{60} ions [15]. The activation energy for the emission of neutral C_2 from C_{60} has been the subject of many studies (see, e.g., Ref. [48] and references therein), where the more recent ones indicate a value of $\sim$10 eV [38,48]. For C_{70} there have been only a few studies [38,49,50], where the most recent measurement [38] indicates a E_a value for neutral C_{70} close to the one for C_{60} (i.e., $\sim$10 eV, or maybe slightly lower). However, activation energies are charge state dependent [15,31], but no data are available beyond those for doubly charged ions [38]. Information on ionization potentials for C_{70} and C_{60} are available up to $r = 5$ [19].

In Fig. 7 we show model fission barriers for C_2^+ emission from C_{70}^{r+} and C_{60}^{r+} as functions of r as calculated through Eq. (2). Here, we have assumed that the C_2 activation energy is independent of r [15], and have used the neutral values of C_{60} and C_{70}, which are $E_a(C_{60}) = 10.3$ eV and $E_a(C_{70}) = 9.5$ eV [38]. These values were obtained from the activation energies of singly charged C_{70}/C_{60} ions and by taking into account the differences in ionization energy between C_{70}/C_{68} and C_{60}/C_{58}, respectively. KER values were calculated by Eq. (2) and were shown in Fig. 6. The ionization potentials for C_{70} and C_{60} used in Eq. (2) were given in Sec. IV B as $I_r = W + (r - 1/2)/a$. The resulting stability limit for $C_{70}(r = 13)$ is slightly larger than the one for $C_{60}(r = 12)$, due

to the somewhat larger model radius for C_{70}.

The highest charged intact C_{60} ions observed experimentally are C_{60}^{12+}, C_{60}^{10+}, and C_{60}^{7+} produced by multiphoton absorption [51], slow highly charged ions [37], and electron bombardment [4], respectively. The most highly charged intact C_{70} ion observed is C_{70}^{10+} from the present study using 69 keV Xe^{23+} projectile ions. There are no theoretical prediction for the C_{70} stability limit, but the ones for C_{60} spread from $r=10$ [52] to $r=13$ [53] and $r=16$ [54]. Emission of C_2^+ appears to dominate for $r>4$ in the case of C_{60} as seen in Fig. 7 and in accordance with observations [5,34,55]. The model results (see Fig. 7) show that the C_{70} fission barriers fall below the C_2 activation energy at slightly higher r values than in the C_{60} case (i.e., evaporation should appear for slightly higher charges for C_{70} than for C_{60}), in accordance with recent experimental observation [56]. In a recent article by Zettergren *et al.* [31] the possible influence of direct C_4^+ emission on the stability limit of multiply charge fullerenes is discussed using the present electrostatic fragmentation model. It is, however, hard to draw firm conclusions from such an analysis as it is very sensitive to the choice of the C_4 model radius.

D. Estimates of lifetimes

We assume a statistical distribution of the internal energies E_n of the ionized fullerenes among the $f=3n-6$ internal vibrational modes (considered to be a collection of independent harmonic oscillators). The classical expression for the probability of localizing enough internal energy in a single mode of an n-atom system and to overcome an energy barrier B is $(1-B/E_n)^{f-1}$. The rate of dissociation then becomes [40,41]

$$k=\tau^{-1}=A\left(1-\frac{B}{E_n}\right)^{f-1}, \tag{3}$$

where τ is the dissociation lifetime and A is the preexponential factor related to a frequency or a characteristic time for the energy equilibration in the system.

The internal energies for C_{60}^{9+} and C_{70}^{10+} ions surviving the relevant experimental time scales are estimated through Eq. (3) with B given by Eq. (2) (assuming that C_2^+ emission dominates). We use $A=2\times10^{19}$ s^{-1} which has been used for the evaporation process of C_{60} and C_{70} [38]. This value is, however, disputed and suggestions range over several orders of magnitude (see, e.g., Refs. [48,57] and references therein).

In order to be observed as an intact fullerene ion (with a certain m/q), the ion must not fragment before leaving the extraction zone. Here the extraction time is $t(C_n^{q+})\approx0.8\sqrt{n/q}$ μs and the fission rate $k(C_n^{q+})$ has to satisfy the condition $k(C_n^{q+})\lesssim1/t(C_n^{q+})$, and we thus obtain typical maximum internal energies of $E_n\approx29$ eV(C_{60}^{9+}) and $E_n\approx30$ eV(C_{70}^{10+}) for ions surviving to the end of the extraction zone. This means that most hotter ions in the initial temperature distribution (with $E_n>30$ eV) have already decayed. The lifetimes of C_{60}^{10+} and C_{70}^{11+} (which has lower barriers B according to Fig. 7 than C_{60}^{9+} and C_{70}^{10+}) will be in the nanosecond range assuming similar internal energies ($\sim$30 eV). For a C_{60}^{10+} ion to survive only an energy of 20 eV would be allowed, that is, the maximum internal energy for surviving in charge state 10+ is higher for C_{70} than for C_{60}. When using Eq. (3) it should be noted that a substantial part of the internal energy E_n is the zero-point or ground-state energy of the fullerene molecules and the remaining part is excitation energy. The zero-point energy can be estimated from the vibrational frequencies for neutral C_{60} calculated by Stanton and Newton [58] with a reduction by 10% [59] yielding 10 eV for C_{60} and 12 eV for C_{70} (scaled from C_{60}).

The estimated maximum excitation energies (C_{60}^{10+}: $30-12=18$ eV, C_{60}^{9+}: $29-10=19$ eV) for surviving the extraction time should be compared to the average excitation energies of C_{60} and C_{70} due to their initial temperature and collisional heating. At the oven temperature of 600°C the average excitation energies are 5.9 eV and 7.0 eV for C_{60} and C_{70}, respectively, as calculated with the vibrational frequencies given in Ref. [58] (with a reduction of 10%) and the Einstein crystal relation. The energies transferred directly in the collision process (through electronic and nuclear energy loss) are estimated to be less than 10 eV even for cases when ten electrons are removed by 69 keV Xe^{23+} ions [28]. In addition, the fullerene ions are indirectly heated when electrons are removed since the fullerene radii increase slightly with increasing charge state. For C_{60}^{12+} this has been estimated to be 3.5 eV [51] and we expect slightly lower values ($\sim$3 eV) for C_{70}^{10+} and C_{60}^{9+}.

Note that the internal energies most likely are larger than B for most values of r shown in Fig. 7. The factor A in Eq. (3) might be slightly different for the two fullerenes, but the exponential dependence on the number of internal degrees of freedom should always dominate. Collisional induced excitation energies are rapidly distributed over the vibrational degrees of freedom and are most likely similar for C_{70} and C_{60} ions produced with the same projectiles and at the same impact parameter ranges. We thus conclude that the lifetime of a C_{70}^{r+} ion is longer than for a C_{60}^{r+} ion with the same internal excitation due to the larger number of vibrational modes for C_{70} on which the excitation energy may be distributed.

V. SUMMARY

In this work, we have presented experimental results on mass spectra for C_{70} and C_{60} fullerenes ionized by slow highly charged ions. This is the first such experimental study, to our knowledge, using a pure C_{70} target, and we report on the so far *highest* charge state (10+) of an intact (on the microsecond time scale) C_{70} ion. Comparison with the C_{60} mass spectra produced under identical conditions strongly indicates that C_{70} ions are inherently more stable than C_{60} ions. The most important evidence for this is the observation of a prominent peak of intact C_{70}^{10+} ion following 69 keV $Xe^{23+}+C_{70}$ collisions, while the C_{60}^{10+} peak is insignificant using the same production method. The apparent production cross section of C_{70}^{9+} is larger than that of C_{60}^{9+} in collisions with Xe^{23+} regardless of the number of ($s=1$, 2, or 3). It should also be mentioned that the production cross section for C_{70}^{5+} is larger than that for C_{60}^{5+} when

Xe^{8+} projectiles are used. The intensity distributions in the fragmentation spectra for C_{60} and C_{70} are rather similar indicating that excitations and following decay processes are quite similar.

KER's for asymmetric fission (C_2^+ emission) are found to be similar for the decays of C_{70}^{r+} and C_{60}^{r+} ions. This behavior is reproduced by a simple electrostatic fragmentation model in which the fragments are treated as conducting spheres. The present experimental KER's are found to be close to previous experimental results for C_{60} ions using slow highly charged ions, while important differences remain in comparison with some results using electron-impact ionization and the MIKE technique [9,10].

The observed larger stability for C_{70}^{r+} ions is rationalized as due to its larger number of internal degrees of freedom (as compared to C_{60}). Estimates of the internal energies for C_{70}^{10+} and C_{60}^{9+} yield results around 30 eV. Assuming the same internal energies for C_{60}^{10+} and C_{70}^{11+}, we arrive at lifetimes in the nanosecond-range, which readily explains why these ions are not observed in the present experiment in spite of their (estimated) finite fission barriers.

ACKNOWLEDGMENTS

We are grateful to Patrik Löfgren, Mikael Blom, and Mikael Björkhage at the Manne Siegbahn Laboratory, Stockholm University, for valuable technical assistance. This work was supported by the Swedish Natural Research Council through Contract Nos. F650-19981278 and F5102-993/2001. The present collaboration was part of the Low Energy Ion Beam Facilities (LEIF) European network, Grant No. HPRI-CT-1999-40012. This work was also supported by the Danish National Research Foundation through the Aarhus Center for Atomic Physics (ACAP).

[1] I. V. Hertel, H. Steger, J. de Vries, B. Weisser, C. Menzel, B. Kamke, and W. Kamke, Phys. Rev. Lett. **68**, 784 (1992).
[2] R. Völpel, G. Hofmann, M. Steidl, M. Stenke, M. Schlapp, R. Trassl, and E. Salzborn, Phys. Rev. Lett. **71**, 3439 (1993).
[3] B. Walch, C. L. Cocke, R. Voelpel, and E. Salzborn, Phys. Rev. Lett. **72**, 1439 (1994).
[4] P. Scheier, B. Dünser, and T. D. Märk, Phys. Rev. Lett. **74**, 3368 (1995).
[5] P. Scheier, B. Dünser, and T. D. Märk, J. Phys. Chem. **99**, 15 428 (1995).
[6] T. Schlathölter, R. Hoekstra, and R. Morgenstern, J. Phys. B **31**, 1321 (1998).
[7] L. Chen, J. Bernard, G. Berry, R. Brédy, J. Désesquelles, and S. Martin, Phys. Scr. **T92**, 138 (2001).
[8] E. E. B. Campbel, K. Hoffmann, and I. V. Hertel, Eur. Phys. J. D **16**, 345 (2001).
[9] S. Matt, B. Dünser, G. Senn, P. Scheier, and T. D. Märk, Hyperfine Interact. **99**, 175 (1996).
[10] G. Senn, T. D. Märk, and P. Scheier, J. Chem. Phys. **108**, 990 (1998).
[11] S. Martin, L. Chen, R. Brédy, J. Bernard, M. C. Buchet-Poulizac, A. Allouche, and J. Désesquelles, Phys. Rev. A **66**, 063201 (2002).
[12] S. Tomita, H. Lebius, A. Brenac, F. Chandezon, and B. A. Huber, Phys. Rev. A **67**, 063204 (2003).
[13] S. Matt, M. Sonderegger, R. David, O. Echt, P. Scheier, J. Laskin, C. Lifshitz, and T. D. Märk, Int. J. Mass. Spectrom. **185**, 813 (1999).
[14] J. Jensen, H. Zettergren, A. Fardi, H. T. Schmidt, and H. Cederquist, Nucl. Instrum. Methods Phys. Res. B **205**, 643 (2003).
[15] H. Cederquist, J. Jensen, H. T. Schmidt, H. Zettergren, S. Tomita, B. A. Huber, and B. Manil, Phys. Rev. A **67**, 062719 (2003).
[16] P. Scheier and T. D. Märk, Int. J. Mass Spectrom. Ion Processes **133**, L5 (1994).
[17] P. Scheier, D. Hathiramani, W. Arnold, K. Huber, and E. Salzborn, Phys. Rev. Lett. **84**, 55 (2000).
[18] R. Wörgötter, B. Dünser, P. Scheier, and T. D. Märk, J. Chem. Phys. **101**, 8674 (1994).
[19] S. Matt, O. Echt, R. Wörgötter, V. Grill, P. Scheier, C. Lifshitz, and T. D. Märk, Chem. Phys. Lett. **264**, 149 (1997).
[20] S. Matt, O. Echt, T. Rauth, B. Dünser, M. Lezius, A. Stamatovic, P. Scheier, and T. D. Märk, Z. Phys. D: At., Mol. Clusters **40**, 389 (1997).
[21] M. Takayama, Int. J. Mass Spectrom. Ion Processes **121**, R19 (1992).
[22] M. Takayama and H. Shinohara, Fullerene Sci. Technol. **2**, 165 (1994).
[23] A. B. Young, L. M. Cousins, and A. G. Harrison, Rapid Commun. Mass Spectrom. **5**, 226 (1991).
[24] T. Nishimura and R. Arakawa, J. Mass Spectrom. **34**, 175 (1999).
[25] K. A. Caldwell, D. E. Giblin, and M. L. Gross, J. Am. Chem. Soc. **114**, 3743 (1992).
[26] H. Shen, P. Hvelplund, D. Mathur, A. Bárány, H. Cederquist, N. Selberg, and D. C. Lorents, Phys. Rev. A **52**, 3847 (1995).
[27] J. Jin, H. Khemliche, M. H. Prior, and Z. Xie, Phys. Rev. A **53**, 615 (1996).
[28] H. Cederquist, A. Fardi, K. Haghighat, A. Langereis, H. T. Schmidt, S. H. Schwartz, J. C. Levin, I. A. Sellin, H. Lebius, B. Huber, M. O. Larsson, and P. Hvelplund, Phys. Rev. A **61**, 022712 (2000).
[29] F. Chandezon, C. Guet, B. A. Huber, D. Jalabert, M. Maurel, E. Monnand, C. Ristori, and J. C. Rocco, Phys. Rev. Lett. **74**, 3784 (1995).
[30] H. Zettergren, H. T. Schmidt, H. Cederquist, J. Jensen, S. Tomita, P. Hvelplund, H. Lebius, and B. A. Huber, Phys. Rev. A **66**, 032710 (2002).
[31] H. Zettergren, J. Jensen, H. T. Schmidt, and H. Cederquist, Eur. Phys. J. D **29**, 63 (2004).
[32] E. E. B. Campbell, T. Raz, and R. D. Levine, Chem. Phys. Lett. **253**, 261 (1996).
[33] L. Chen, J. Bernard, A. Denis, S. Martin, and J. Désesquelles, Phys. Rev. A **59**, 2827 (1999).
[34] S. Martin, L. Chen, A. Denis, R. Brédy, J. Bernard, and J. Désesquelles, Phys. Rev. A **62**, 022707 (2000).

[35] S. Tomita, H. Lebius, A. Brenac, F. Chandezon, and B. A. Huber, Phys. Rev. A **65**, 053201 (2002).
[36] S. Martin, L. Chen, A. Denis, and J. Désesquelles, Phys. Rev. A **59**, R1734 (1999).
[37] A. Brenac, F. Chandezon, H. Lebius, A. Pesnelle, S. Tomita, and B. A. Huber, Phys. Scr. **T80**, 195 (1999).
[38] S. Tomita, J. U. Andersen, C. Gottrup, P. Hvelplund, and U. V Pedersen, Phys. Rev. Lett. **87**, 073401 (2001).
[39] C. Bréchignac, P. Cahuzac, F. Carlier, J. Leygnier, and A. Sarfati, Phys. Rev. B **44**, 11 386 (1991).
[40] O. K. Rice and H. C. Ramsperger, J. Am. Chem. Soc. **49**, 1617 (1927).
[41] L. S. Kassel, J. Phys. Chem. **32**, 225 (1928).
[42] U. Näher, S. Bjørnholm, S. Frauendorf, F. Garcias, and C. Guet, Phys. Rep. **285**, 245 (1997).
[43] N. G. Gotts and A. J. Stace, Phys. Rev. Lett. **66**, 21 (1991).
[44] W. A. deHeer and P. Milani, Phys. Rev. Lett. **65**, 3356 (1990).
[45] C. J. Reid, J. A. Ballestine, S. R. Andrews, and F. M. Harris, Chem. Phys. **190**, 113 (1995).
[46] I. Compagnon, R. Antoine, M. Broyer, P. Dugourd, J. Lermé, and D. Rayane, Phys. Rev. A **64**, 025201 (2001).
[47] O. V. Boltalina, I. N. Ioffe, L. N. Sidorov, G. Seifert, and K. Vietze, J. Am. Chem. Soc. **122**, 9745 (2000).
[48] S. Matt, O. Echt, P. Scheier, and T. D. Märk, Chem. Phys. Lett. **348**, 194 (2001).
[49] S. Matt, O. Echt, R. Wörgötter, P. Scheier, C. E. Klots, and T. D. Märk, Int. J. Mass Spectrom. Ion Processes **167**, 753 (1997).
[50] P. E. Barran, S. Firth, A. J. Stace, H. W. Kroto, K. Hansen, and E. E. B. Campbell, Int. J. Mass Spectrom. Ion Processes **167**, 127 (1997).
[51] V. R. Bhardwaj, P. B. Corkum, and D. M. Rayner, Phys. Rev. Lett. **91**, 203004 (2003).
[52] J. Cioslowski, S. Patchkovskii, and W. Thiel, Chem. Phys. Lett. **248**, 116 (1997).
[53] T. Bastug, P. Kurpick, J. Meyer, W. D. Sepp, B. Fricke, and A. Rosen, Phys. Rev. B **55**, 5015 (1997).
[54] G. Seifert, R. Gutierrez, and R. Schmidt, Phys. Lett. A **211**, 357 (1996).
[55] S. Martin, L. Chen, A. Denis, and J. Désesquelles, Phys. Rev. A **57**, 4518 (1998).
[56] J. Jensen, H. Zettergren, H. T. Schmidt, and H. Cederquist (unpublished).
[57] C. Lifshitz, Int. J. Mass Spectrom. Ion Processes **198**, 1 (2000).
[58] R. E. Stanton and M. D. Newton, J. Phys. Chem. **92**, 2141 (1988).
[59] R. K. Yoo, B. Ruscic, and J. Berkowitz, J. Phys. Chem. **96**, 911 (1992).